Journal of Nuclear Materials 390–391 (2009) 568–571

Contents lists available at ScienceDirect

Journal of Nuclear Materials

journal homepage: www.elsevier.com/locate/jnucmat

Ion implanted deuterium retention and release from clean and oxidized beryllium

M. Reinelt, Ch. Linsmeier *

Max-Planck-Institut für Plasmaphysik, EURATOM Association, Boltzmannstrasse 2, 85748 Garching b. München, Germany

ARTICLE INFO

PACS:
52.40.Hf
68.43.Vx
61.80.Jh
66.30.je
79.20.Rf

ABSTRACT

The deuterium retention and thermal recycling behavior of clean and oxide-covered beryllium is investigated by a combination of temperature programmed desorption, X-ray photoelectron spectroscopy and other methods. From the experimental results, the retention mechanisms are deduced and activation energies for the release processes are obtained from modeling. Implanted deuterium at 1 keV kinetic energy is trapped locally in ion-induced defects with a release temperature above 700 K. At a local deuterium concentration greater than 0.35 D/Be, the beryllium bulk is supersaturated. This leads to the formation of additional binding states with a release temperature of 450 K and formation of BeD_2, which decomposes at 570 K. The amount of deuteride formed is influenced by the target temperature during implantation. The Be surface and BeO surface layers have no rate-limiting influence on the thermal release process.

1. Introduction

The main wall of ITER's plasma vessel is planned to be covered with beryllium as a plasma-facing material [1]. During operation, intense fluxes of hydrogen isotopes are implanted and retained in the plasma-facing material. Sputtering and high temperature lead to a release of retained hydrogen into the plasma or transport inside the component. Especially from a safety point of view, a detailed knowledge on the hydrogen recycling behavior in Be is needed to predict the machine's total tritium inventory. For this, characteristic values describing the recycling like diffusivity, solubility and detrapping energies are needed. Usually, these values are gained from modeling experimental data. Although a large number of studies have been dedicated to this issue in the past, the details of the mechanisms governing the retention are still unclear. This can be seen primarily in a large scatter of the characteristic values. Even the reported retained areal densities vary up to two orders of magnitude [2]. Three possible reasons should be considered.

1.1. Sample crystallinity

The defect density or grain size distribution of the Be samples under investigation can have a significant influence on the trap site density or diffusivity of hydrogen. As quantitative results require modeling, uncertainties in the sample structure can lead to misinterpretation of experimental data. The experiments described in this work are performed with single crystalline Be. Defects created in the course of the experiments are annealed by temperature treatment assuring the structural integrity of the sample.

1.2. Chemical composition of the Be surface

Be reacts very quickly with oxygen or water forming a closed BeO surface layer even under good vacuum conditions [3]. Because the release process of implanted hydrogen has to occur via the substrate surface, the chemical condition of the surface can have a significant influence. It can introduce an additional energy barrier for coverages even below one monolayer (ML). This is especially important for permeation or, as in this work, for desorption experiments, where a superposition of all (release-) rate-limiting processes is measured. Up to now, no experimental data for hydrogen retention implanted into oxygen-free Be (i.e. Be without a BeO-covered surface) was reported.

1.3. Retention mechanisms

In order to extract quantitative results from experiments involving the temperature-driven transport of hydrogen inside and out of beryllium metal by modeling, the rate-limiting steps have to be identified. Evaluation of experimental data of the temperature-dependent release of hydrogen requires the assignment of observed peaks to rate-limiting mechanisms such as detrapping, diffusion or recombination ($2D \rightarrow D_2$).

2. Experimental

The Be sample under investigation is a single crystalline disk with a diameter of 14 mm and a thickness of 0.5 mm. The single

* Corresponding author.
E-mail addresses: matthias.reinelt@ipp.mpg.de (M. Reinelt), linsmeier@ipp.mpg.de (Ch. Linsmeier).

0022-3115/$ - see front matter © 2009 Elsevier B.V. All rights reserved.
doi:10.1016/j.jnucmat.2009.01.103

crystallinity is confirmed by Laue diffractography and shows an orientation of the mirror-polished surface of $(11\bar{2}0)$ with a misscut of less than 1°. The surface of the Be sample is cleaned under UHV conditions by cycles of bombardment with a scanned 3 keV Ar^+ ion beam 45° to the surface at room temperature and subsequent annealing up to 1000 K. The chemical surface composition is monitored by X-ray photoelectron spectroscopy (XPS) and low energy ion scattering spectroscopy (LEIS). LEIS is performed with a 480 eV He ion beam at a scattering angle of 135°. A minimal residual oxide coverage of 0.2 ML on the sample surface as the only contamination could be achieved and maintained for 12 h at a base pressure of 2×10^{-11} mbar. The cleaned sample is bombarded by a mass-separated, monoenergetic 3 keV D_3^+ ion beam under perpendicular angle of incident. This corresponds to a kinetic energy of 1 keV per deuterium atom. TPD experiments are performed by heating the sample at a linear ramp with electron impact from the back. The sample temperature is measured by a thermocouple spot-welded to the sample surface at a position where it is not irradiated by the ion beams. The effusing gas flux is detected by a differentially pumped quadrupole mass spectrometer (QMS) in the line-of-sight geometry. The amount of surface oxide does not change during implantation and TPD experiments. The deuterium flux is calibrated by measuring the retained deuterium areal density after implantation in situ by nuclear reaction analysis (NRA). The reaction $D(^3He,p)^4He$ with 800 keV $^3He^+$ ions from a 3 MV tandem accelerator is used [4]. After TPD experiments up to 1000 K, no residual D can be detected in the sample both by NRA, and by successive TPD runs. Desorption of oxygen-containing molecules such as HDO and D_2O is not observed. The flux of HD formed during desorption is two orders of magnitude lower than the effusing D_2 flux and is therefore ignored in the following. All experiments, except scanning electron microscopy (SEM) shown in Fig. 1(b) and (c) are performed in situ in an experimental setup described elsewhere in detail [5].

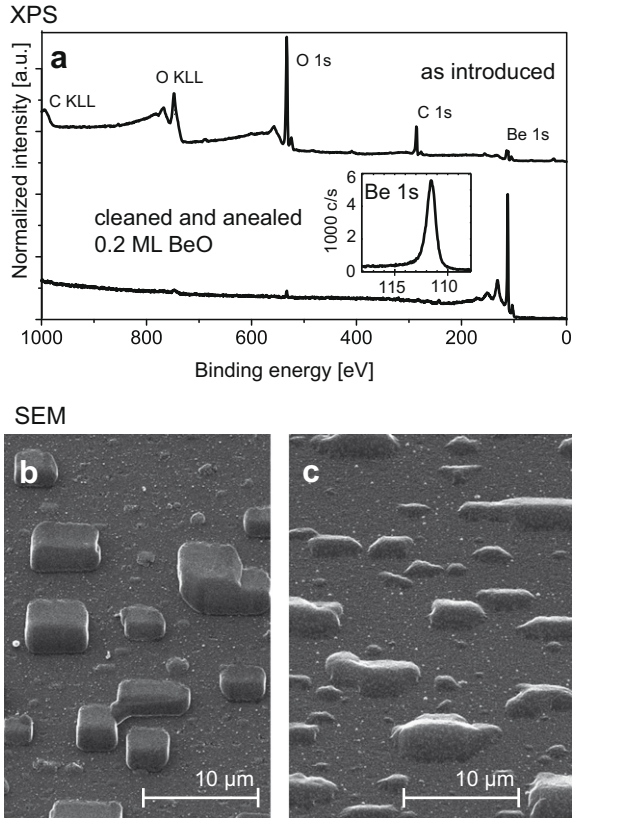

Fig. 1. In situ XPS spectra of the Be sample, as introduced and after cleaning and annealing. The insert shows the Be 1s binding energy region of the clean, annealed and D-implanted Be surface (a). Ex situ SEM image of the annealed Be sample (b). Ex situ SEM image of the cyclically sputtered (Ar ions) and annealed sample surface (c).

3. Results

3.1. Substrate characterization

Fig. 1(a) shows normalized XPS spectra of the Be sample surface as introduced (upper spectrum) and after many cleaning and annealing cycles (lower spectrum). The residual oxygen contamination of the cleaned sample surface corresponds to an equivalent of 0.2 monolayers BeO. The insert shows the photoelectron peak of the Be 1s binding energy region of the cleaned sample. The binding energy is 111.8 eV of the clean metal. Although the Be sample is originally a single crystal, its near-surface region is severely damaged by the Ar bombardment of the cleaning process. Flash heating the sample up to 1000 K can anneal these defects and recrystallize the sample surface. By this procedure, implanted Ar is also removed from the near-surface region. TPD spectra after temperature treatment up to 1000 K show no desorbing gaseous species from the sample (Ar or hydrogen in any form). The effect of the recrystallization is directly visible by SEM imaging (Fig. 1(b)) on the sample surface, which was heated cyclically from RT to 1000 K under UHV conditions (without ion bombardment). Micrometer-sized facetted Be crystallites are formed on the initially flat sample surface. The uniform alignment of the facetted structures across the whole sample additionally indicates the single crystallinity of the bulk material. The 30° tilted facets have an orientation of $(10\bar{1}0)$. The sides (left and right of each crystallite in Fig. 1(b)) are oriented (0001). Driving force of this mass transport is the minimization of the surface energy. Electron backscattering diffraction (EBSD) shows that the crystallographic structure and orientation of the crystallites and original sample surface are identical, which means that the crystal develops a facetted surface under these conditions without loosing the bulk single crystallinity. Cycles of ion bombardment and annealing lead to a roughening of the surface by recrystallization and simultaneous erosion of the recrystallized structures (Fig. 1(c)) This roughness increases the (flat) projected surface area of the irradiated surface region up to a factor of 1.2, as measured by atomic force microscopy (AFM). LEIS measurements after increasing annealing temperatures show, that Be from the bulk segregates through thin BeO surface layers, forming a (metallic) Be-terminated surface above a temperature of 900 K. The original BeO surface layer is thus covered by at least one ML of metallic Be. This surface is stable at lower temperatures, until oxidized by residual gas. Such a mechanism is in agreement with results from ^{18}O marker experiments performed by Roth et al. [6]. On the basis of those observations, the conclusions can be drawn that annealing of the cleaned Be sample leads to a recrystallization of the surface. The chemical surface composition and sample crystallinity are therefore well defined for thermal release experiments of implanted deuterium.

3.2. Deuterium retention mechanism at fluences below 1.0×10^{21} m^{-2}

A TPD spectrum ($m/q = 4$, D_2) of implanted D reveals several release steps (Fig. 2(a) and (b)). Below fluences of 1.0×10^{21} m^{-2}, D is trapped in two types of bulk sites, related to defects created by the implantation cascade with release temperatures of 780 and 850 K (denoted as release states 1 and 2 in Fig. 2). Fig. 2(a) shows a TPD spectrum after bombarding the sample at RT with a fluence of 6.5×10^{20} m^{-2}. A lateral scan of the sample with NRA reveals

a D distribution similar to the intensity profile of the implantation beam. The release from the ion-induced trap sites involves detrapping to a solute (mobile) state, diffusion through the bulk lattice, recombination to molecular D_2 at the surface and finally desorption into vacuum. All steps can influence the observed peak temperature, although detrapping is the rate-limiting step. To include all these processes into a model, TMAP7 is used [7]. This code includes diffusive and surface processes. For the model, the diffusivity from Abramov et al. [8] is used. It is given as $6.7 \times 10^{-9}\exp(-0.29\ \text{eV}/kT)\ [\text{m}^2\ \text{s}^{-1}]$, which corresponds to a diffusion length of micrometers (per second) already at room temperature. The solubility is taken from Shapovalov and Dukel'ski [9] and the surface recombination barrier for D on pure Be as 0.87 eV from Lossev and Küppers [10]. The D concentration profile is taken from a static SDTrim.SP calculation, a Monte Carlo code that can model kinematic processes of ion implantation into a solid material [11]. A manual adjustment of the calculated desorption flux to the TPD experiments yields activation energies of 1.88 eV and 2.05 eV for the detrapping from the ion-induced sites (1) and (2).

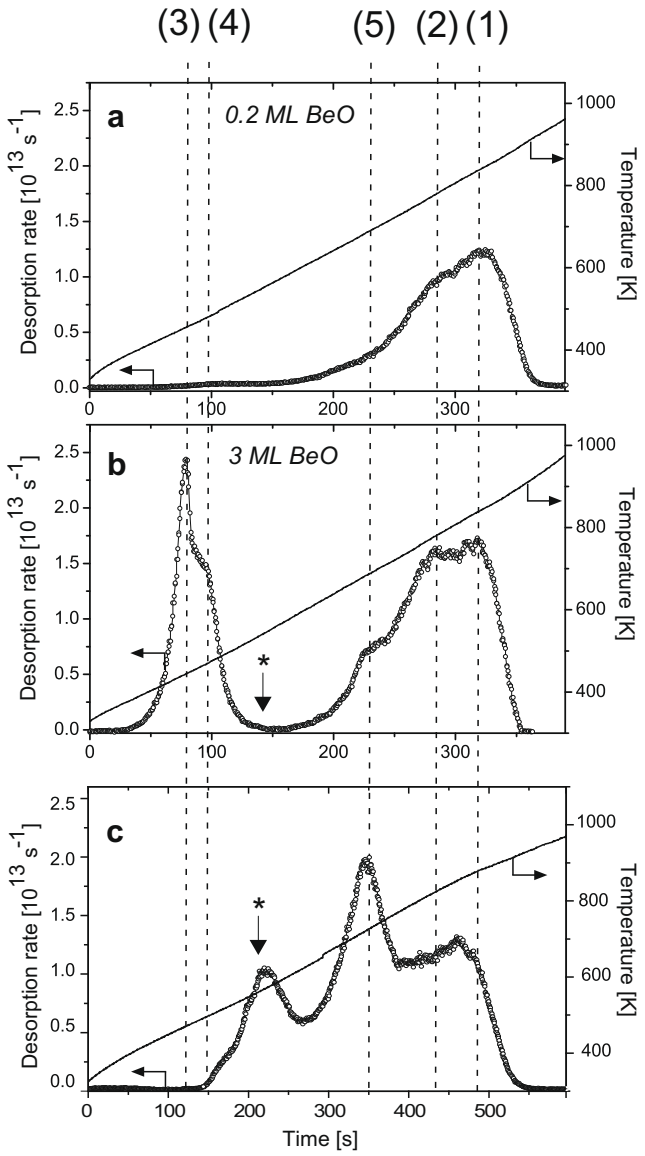

Fig. 2. TPD spectra ($m/q = 4$, D_2) after implantation of different deuterium fluences: (a) $6.5 \times 10^{20}\ \text{m}^{-2}$ and (b) $1.8 \times 10^{21}\ \text{m}^{-2}$. The asterisk indicates the decomposition temperature of BeD_2. The spectrum (c) is recorded after implantation at a substrate temperature of 530 K.

3.3. Deuterium retention mechanism at higher fluences

Above a fluence of $1.0 \times 10^{21}\ \text{m}^{-2}$ (Fig. 2(b)), additional binding states with release temperatures of 440 K and 480 K are created due to a D accumulation in the bulk. These binding states show a sharp threshold behavior and appear only above an irradiation fluence of $1.0 \times 10^{21}\ \text{m}^{-2}$. In Fig. 2(b) these states are denoted as (3) and (4). The local supersaturation enforces nanoscaled structural modifications in the Be lattice. Release from these states is energetically different from detrapping from states (1) and (2), resulting in a lower peak temperature. Simulations of a first order release reaction [12] with a frequency factor of $10^{13}\ \text{s}^{-1}$ by a rate equation yield activation barriers of 1.25 eV and 1.33 eV for states (3) and (4), respectively. Above the threshold fluence for the appearance of release peaks (3) and (4), SEM and AFM images show protrusions on the D-irradiated sample surface with a size of about 100 nm. Cracking of the surface is not observed. Depth profiles from SDTrim.SP calculations, which allow an accumulation of D in the Be bulk show, that D reaches a local concentration of 0.26 at.% in a depth of 40 nm at an irradiation fluence of $1.0{\cdot}10^{21}\ \text{m}^{-2}$. This corresponds to a maximum Be/D ratio of 0.35, which is in the range of values for the maximum D concentration given in previous studies [2]. The sample retention reaches steady-state at irradiation fluences above $2.0 \times 10^{21}\ \text{m}^{-2}$, where 30% of the retained amount is trapped in the supersaturated states. The maximum retained areal density is $2.0 \times 10^{21}\ \text{m}^{-2}$. This is in good agreement to earlier investigations by Haasz and Davis [13].

3.4. Influence of a thin BeO surface layer

To investigate the influence of a BeO-covered surface, the sample is thoroughly cleaned, annealed and implanted with deuterium. XPS shows an oxygen contamination equivalent to 0.2 monolayers BeO on the surface after the implantation. The sample is stored overnight under UHV conditions to allow the growth of a closed BeO surface layer of 3 monolayer thickness from the residual gas (reactive species: water). A successive TPD experiment is directly compared with an experiment with the same cleaning procedure and irradiation fluence, but TPD immediately after the implantation. For the first experiment, all desorption occurs via the BeO-covered surface, while for the latter, the surface is fully Be-terminated, as discussed above. Any difference in the spectra can hence be directly related to the influence of the oxide coverage. The segregation of metallic Be to cover the BeO surface layer during the temperature ramp of the TPD experiment occurs above 900 K, where D is already released from the sample. Assuming that D_2 (as a molecule) does not diffuse through the Be lattice, the last step for the release processes of any retained D is recombination to D_2 on the sample surface. If the chemical surface composition is changed from Be to BeO, the energetic conditions change for this step. The recombination process itself can be limited, for example, by the surface diffusivity for adsorbed D atoms and its activation barrier. Changing the chemical composition of the outermost ML would consequently result in a shift of the measured temperature of any release peak limited by such a recombination process. The experiments show, however, that none of the peaks (1)–(4) is influenced by the chemical composition of the surface, hence none of the peaks is recombination-limited. Instead, increased amounts of D are released from state (5) in the TPD experiment with oxide-covered beryllium. Since the amount released in peak (5) is influenced by the areal density of BeO, it is concluded that D is bound to BeO on the surface, presumably as a hydroxide.

3.5. Implantation at elevated temperature

Elevated substrate temperatures during implantation can alter the retention mechanism. To investigate the influence of elevated substrate temperatures on the retention mechanisms, the sample is kept at 530 K during implantation. The substrate temperature is, hence, above the release temperatures of states (3) and (4). As a consequence, these states cannot be occupied at fluences above $1 \times 10^{21}\ m^{-2}$. The chemical surface composition is monitored by XPS and does not change during the experiments. A successive TPD experiment (Fig. 2(c)) starting at room temperature shows a peak at 570 K, which is a dominant release peak in this case (its position is indicated by an asterisk in Fig. 2). Also, increased amounts are released at 680 K, the decomposition temperature of the surface hydroxide. The ion-induced trap sites (1) and (2) are not affected in position and occupation by the increased substrate temperature. A possible explanation for the formation of surface hydroxide despite the constant clean sample surface in the irradiation zone, is an increased diffusivity of D during the implantation. This allows D to reach (uncleaned) outer sample regions or the sample back to form the hydroxide. Although states (3) and (4) are not occupied at implantation temperatures above 500 K, the retention of the sample is not reduced proportionally. Deuterium, which is bound in the supersaturated areas at room temperature implantation, is instead bound to a state with a release temperature of 570 K. This can be explained by the increased substrate temperature, which allows a phase formation of beryllium deuteride BeD_2 upon local supersaturation of the bulk during the implantation. It is reported that BeH_2 (and accordingly BeD_2, under the assumption of similar isotope behavior) decomposes above 570 K [14], which is the dominant release temperature observed in this experiment. A chemical shift of the Be 1s binding energy due to the hydride formation [15] is not observed by XPS, which indicates that the hydride is formed below the information depth of XPS. This is consistent with the formation of the hydride in the supersaturation zone in a depth of 40 nm, which is well beyond the XPS information depth of about 20 nm.

4. Summary

The investigation of deuterium retention by a combination of TPD and surface analytical techniques reveals qualitatively the retention mechanisms and release processes of deuterium implanted into beryllium. This allows modeling of the experimental results and thus obtaining quantitative values such as activation energies. At low fluences, deuterium is trapped in ion-induced defects. The release from these binding states has activation barriers of 1.88 eV and 2.05 eV, respectively. Above a fluence of $1 \times 10^{21}\ m^{-2}$, which corresponds to a local concentration of 0.35 D/Be in a depth of 40 nm, local supersaturation of the bulk leads to the creation of binding states with a lower release temperature similar to surface desorption. The activation energies for the release from these states are 1.25 eV and 1.33 eV, respectively for a first order release-reaction mechanism. With increasing implantation temperature, implanted D above the saturation concentration forms increasing amounts of BeD_2, which decomposes again above 570 K. The sample surface (metallic Be or BeO) has no rate-limiting influence on the thermal release, because all deuterium implanted with an energy of 1 keV is retained and released from binding states in the bulk.

References

[1] G. Federici, R. Anderl, J.N. Brooks, R. Causey, J.P. Coad, D. Cowgill, R. Doerner, A.A. Haasz, G. Longhurst, S. Luckhardt, D. Mueller, A. Peacock, M. Pick, C.H. Skinner, W. Wampler, K. Wilson, C. Wong, C. Wu, D. Youchison, Fus. Eng. Des. 39&40 (1998) 445.
[2] R.A. Anderl, R.A. Causey, J.W. Davis, R.P. Doerner, G. Federici, A.A. Haasz, G.R. Longhurst, W.R. Wampler, K.L. Wilson, J. Nucl. Mater. 273 (1999) 1.
[3] S. Zalkind, M. Polak, N. Shamir, Surf. Sci. 385 (1997) 318.
[4] V.K. Alimov, M. Mayer, J. Roth, Nucl. Instrum. and Meth. B 234 (2005) 169.
[5] Ch. Linsmeier, P. Goldstrass, K.U. Klages, Phys. Scr. 2001 (2001) 28.
[6] J. Roth, W.R. Wampler, W. Jacob, J. Nucl. Mater. 250 (1997) 23.
[7] J.A. Ambrosek, G.R. Longhurst, INEEL/EXT-04-01657, 2004.
[8] E. Abramov, M.P. Riehm, D.A. Thompson, W.W. Smeltzer, J. Nucl. Mater. 175 (1990) 90.
[9] V.I. Shapovalov, Y.M. Dukel'ski, Russ. Met. 5 (1984) 210.
[10] V. Lossev, J. Küppers, Surf. Sci. 284 (1993) 175.
[11] W. Eckstein, Computer Simulation of Ion–Solid Interactions, Springer-Verlag, Berlin, 1991.
[12] A.M. de Jong, J.W. Niemantsverdriet, Surf. Sci. 233 (1990) 355.
[13] A.A. Haasz, J.W. Davis, J. Nucl. Mater. 241–243 (1997) 1076.
[14] P.E. Barry, J.S. Bowers, R.G. Garza, P.C. Souers, J.S. Cantrell, T. Beiter, J. Nucl. Mater. 173 (1990) 142.
[15] G. De Temmerman, M.J. Baldwin, R.P. Doerner, D. Nishijima, R. Seraydarian, K. Schmid, J. Nucl. Mater. 390–391 (2009) 564.